Organic LETTERS

Letter

pubs.acs.org/OrgLett

Synthesis, Structure, and Opto-electronic Properties of Regioisomeric Pyrene−Thienoacenes

Shiqian Zhang,[†] Xiaolan Qiao,[‡] Ying Chen,[†] Yuanyuan Wang,[†,‡] Robert M. Edkins,[§] Zhiqiang Liu,*[,†] Hongxiang Li,*[,‡] and Qi Fang[†]

[†]State Key Laboratory of Crystal Materials, Shandong University, Jinan 250100, China

[‡]Shanghai Institute of Organic Chemistry, Chinese Academy of Sciences, Shanghai 200032, China

[§]Institut für Anorganische Chemie, Julius-Maximilians-Universität Würzburg, Am Hubland, 97074 Würzburg, Germany

Supporting Information

ABSTRACT: Three regioisomeric sulfur-bridged pyrene−thienoacenes (PTAs) have been synthesized. The crystal structures and optoelectronic properties of these ring-fused PTAs and their ring-opened precursors have been fully investigated. Among these isomers, the [3,4]-extended compound (4-S-PTA) shows the most pronounced spectral red-shift and highest quantum yield as well as large transistor mobility.

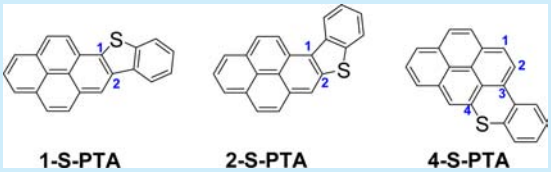

From the viewpoint of both organic synthesis and optoelectronic properties, the chemistry of pyrene is strongly position-dependent.[1] The 1-, 3-, 6-, and 8-positions of pyrene can be regarded as "common sites", which are known as the most active sites for electrophilic aromatic substitution (S_EAr) reactions, and most pyrene derivatives are extended from these positions.[1,2] Among the other "un-common sites", the 2- and 7-positions of pyrene are known as the molecular node sites and are extremely difficult to derivatize by ordinary methods, except where steric hindrance precludes reactions at the common sites (e.g., Friedel−Crafts *tert*-butylation[3]). The finding of Marder et al. that Ir-catalyzed direct borylation of pyrene is highly selective for the 2- and 7-positions has opened up a new way to functionalize pyrene.[4,5] At the 4-, 5-, 9-, and 10-positions, which are also defined as the K-region of pyrene, oxidation can take place,[6] and the reaction has recently been extended by Müllen et al. prior to unsymmetrical bromination at the 9- and 10-positions.[7] Itami and co-workers have also reported that Pd-catalyzed oxidative direct arylation can asymmetrically functionalize pyrene at the 4-position.[8]

Although much work has focused on functionalizing pyrene derivatives at the "common" or "un-common" sites, regioselective synthetic strategies and their opto-electronic properties need to be considered carefully.[9,10] To our knowledge, although many sulfur-containing heteroaromatics,[11] such as naphthothiophenes and anthrathiophenes, show excellent semiconducting performance,[12,13] few pyrene−thienoacenes (**PTA**) have been reported.[7,14] Considering the nature of both extensive intramolecular π-conjugation and strong intermolecular π-stacking of pyrene itself,[1a] well-designed pyrene-based thienoacenes should be able to fit the structural requirments of organic semiconductors.

Herein, we present the syntheses, crystal structures, and photophysical properties of three isomeric **PTAs** and their precursors, which are greatly dependent on the position of substitution on the pyrene skeleton.

As illustrated in Scheme 1, the **PTAs** were synthesized via different routes with good yields. The acid-induced cyclization of aromatic methyl sulfoxides, which has been developed by Müllen et al.[15] and extended by others to synthesize thienoacenes,[12,16] is the key step of this process. For the synthesis of precursors **S-X-S** (**X** = 1, 2, or 4), which also serve as open-ring analogues of **PTAs** for comparison studies, the Suzuki−Miyaura cross-coupling between appropriate boronates and aryl halides were adopted. The coupled product was oxidized using H_2O_2 to generate the sulfoxide intermediates, which can be used directly in the next step. Finally, the target **PTAs** were obtained by treating the sulfoxide intermediates with trifluoromethanesulfonic acid and subsequent demethylation in water/pyridine mixture.

Because the stability of aromatic thiophene is much better than the sulfur-bridged 6-membered rings, most of the reported products of this acid-induced cyclization are sulfur-bridging 5-membered-ring-fused thienoacenes. In this work, **1-S-PTA** was prepared as expected with good yield from compound **2** using the approach outlined above. Thus, compound **4** might be expected to bring about **2-S-PTA**. However, X-ray crystallographic analysis of the cyclization product indicated that the sulfur atom is bonded to the 4-position rather than 2-position of pyrene; i.e., it is **4-S-PTA**. This may be due to the fact that the 2-position lies in the nodal plane of both the HOMO and LUMO of pyrene,[4] making it the most inert site.

To synthesize **2-S-PTA** for comparison studies, first *ortho*-lithiated 1-methoxypyrene (**5**) was reacted with dimethyl disulfide (Me_2S_2) to give 1-methoxy-2-methylthiopyrene (**6**) in nearly quantitative yield. After selective demethylation of the methoxy groups and subsequent triflation to give compound **7**, the Suzuki−Miyaura coupling with phenylboronic acid afford **S-**

Received: October 15, 2013
Published: January 3, 2014

Scheme 1. Synthetic Approach to Isomers of PTAs

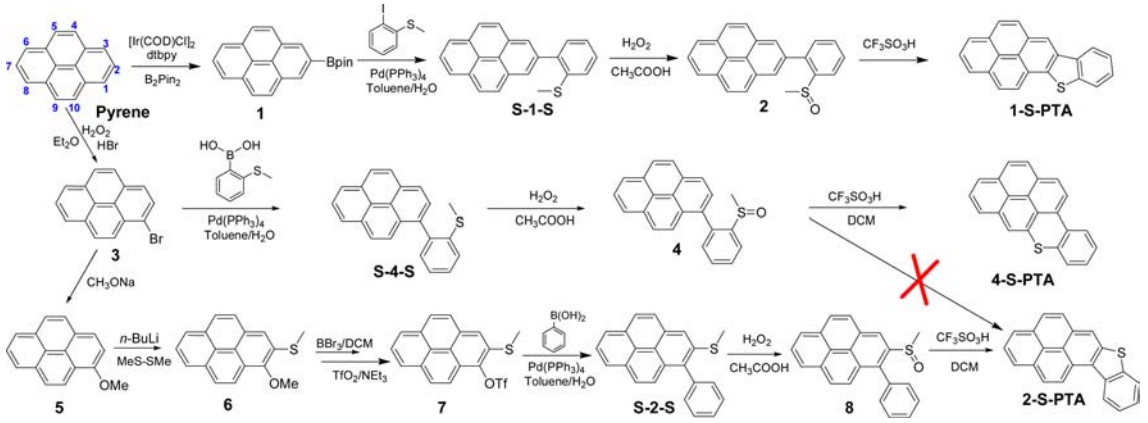

2-S. Oxidation and then acid-induced cyclization of **8** worked smoothly to afford **2-S-PTA** as expected.

It should be noted that when **4** or **8** were treated with neat CF_3SO_3H as in a reported procedure,[16] only low yields of the desired cyclization products were obtained. This may be due to the lower activity of position 4 and 2- of pyrene than that of position 1 and also the possibility of competitive intermolecular[17]and intramolecular[15] coupling reactions of aromatic methyl sulfoxide with activated aromatic building blocks to produce high-molecular weight polymers or cyclization products. To synthesize **2-S-PTA** and **4-S-PTA**, predissolving **8** and **4**, respectively, in a solvent such as DCM or chloroform was necessary.

All of the isomers were characterized fully by ^1H NMR, $^{13}C\{H\}$ NMR, and high-resolution MS and their structures were obtained by single-crystal X-ray diffraction. All compounds exhibit good thermal and oxidative stability in air. The melting points of these **PTAs** are generally 30−50 °C higher than those of the corresponding **S-X-S**, presumably due to the improved molecular rigidity and enhanced $\pi-\pi$ interaction.

Single crystals of the **PTAs** and their precursor **S-X-S** were grown by slow evaporation from solutions. All of the **S-X-S** compounds display significantly twisted structures with large torsion angles of ca. 80° between the pyrene and phenyl rings (76.40° for **S-1-S**, 82.58° for **S-2-S**, and 82.67° for **S-4-S**). However, all of the **PTAs** display nearly planar structures (see the side view in Figure 1), the torsion angle between the fused pyrene and phenyl rings is only 1.34° for **1-S-PTA** and 4.0° for **2-S-PTA**. The 6-membered ring-fused **4-S-PTA** has the largest torsion angle, which is only 6.21°. In addition, comparing the bond length of the C−C bond connecting the phenyl and pyrenyl moieties, the bond length of **PTAs** are reduced more or less than those of **S-X-S**, for example, 1.493 vs 1.459 Å (**S-1-S** vs **1-S-PTA**), 1.488 vs 1.476 Å (**S-2-S** vs **2-S-PTA**), and 1.506 vs 1.492 Å (**S-4-S** vs **4-S-PTA**), which indicate the relative less $\pi-\pi$ conjugation of **S-X-S** than corresponding ring-fused **PTAs**.

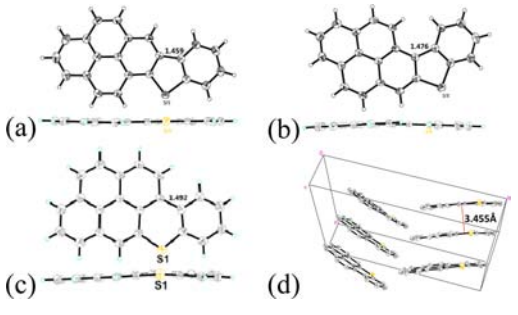

Figure 1. Molecular structures of **1-S-PTA** (a), **2-S-PTA** (b), and **4-S-PTA** (c) and packing diagram of **4-S-PTA** (d).

1-S-PTA and **2-S-PTA** crystallized in the monoclinic space groups $P2_1/c$ and $P2_1$, respectively, and **4-S-PTA** crystallized in orthorhombic space group $P2_12_12_1$. The **PTAs** adopt face-to-face column and herringbone-like structures in the crystals, and strong intermolecular $\pi-\pi$ and C−H···π interactions are observed. **4-S-PTA** possesses the shortest $\pi-\pi$ distance of 3.455 Å, and the $\pi-\pi$ distance is 3.55 Å for **1-S-PTA** and 3.54 Å for **2-S-PTA**. In addition, the $\pi-\pi$ overlap area of **2-S-PTA** is close to that of **4-S-PTA** but larger than that of **1-S-PTA**.

The most interesting point is that the photophysical properties of **PTAs** and **S-X-S** clearly indicate that the $\pi-\pi$ conjugation in these pyrene−benzene systems greatly depends on the position of substitution on the pyrene skeleton. Generally, the absorption spectra of **S-X-S** are quite similar to those of pyrene (Figure S-3, Supporting Information) maintaining the well-resolved vibronic structures, albeit with small red-shift (Figure 2). However, the absorption of **PTAs** is

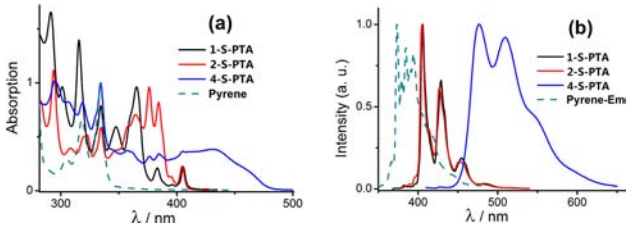

Figure 2. Normalized absorption (a) and fluorescence emission (b) spectra of **PTAs** in hexane.

greatly red-shifted compared to **S-X-S**; i.e., there is a decrease of the optical band gap as result of the ring-fusion. All of the absorption spectra of the **PTAs** have a peak at 334 nm with a pronounced vibronic progression, which is similar to the $S_0 \rightarrow S_2$ transition of pyrene. However, the absorption bands in 350−500 nm are greatly extended with different structures. Because both the HOMO and LUMO of unsubstituted pyrene have nodal planes passing through the 2- and 7-positions, there tends to be less interaction of these orbitals with substitutents at these positions in the pyrene derivatives. However, substitution at positions 1- (or equivalently 3-) and 4- of pyrene allow stronger interactions with both the HOMO and LUMO. **4-S-PTA** has

dx.doi.org/10.1021/ol402971n | Org. Lett. 2014, 16, 342−345

substituents at both C3 and C4, so the absorption band of the 3,4-extended **4-S-PTA** is even greatly red-shifted to 480 nm. This also indicates the band gap of **4-S-PTA** is much narrow than those of other isomers.

TD-DFT-calculated singlet excitations (B3LYP and CAM-B3LYP/6-311G(d), vacuum) were used to rationalize the absorption spectra (Figures S-37−S-39 and Tables S-4−S-9, Supporting Information). Both functionals predict the same order of the lowest excited states with similar orbital descriptions but different energies and oscillator strengths. The red-shift of **4-S-PTA** relative to **1**- and **2-S-PTA** is due to destabilization (ca. 0.3 eV) of the HOMO by the donor S atom at the 4-position. **1-S-PTA** has a higher lying LUMO (by ca. 0.2 eV) than the other isomers, due to reduced conjugation between the pyrene and phenyl rings bonded through the pyrene 2-position, shifting its absorption to higher energy.

The fluorescence emission of the **PTAs** depends on the excitation wavelength (Figures S-8−S-13 and Table S-3, Supporting Information). When they are excited at 334 nm, they exhibit emission similar to that of pyrene; however, when excited at longer wavelengths, their emission spectra are shown red-shifted with a clear, pronounced vibronic structure. The fluorescence lifetimes also indicated there are two different emissive excited states involved in the 334 nm excitation. Correspondingly, the quantum yields are also excitation-dependent. **4-S-PTA** possesses the highest quantum yields as high as 0.60.

As determined by cyclic voltammetry (CV), all these **PTAs** show a single reversible oxidation wave at about 0.80 eV vs Ag/AgCl (Table 1 and Figure 3a).

Table 1. Opto-electronic Properties of S-X-S and PTAs.[a]

	λ_{abs}[b] (nm) (log ε)	λ_{em}[c] (nm)	Φ[d]	τ[e] (ns)	E_{ox}[f] (eV)
S-1-S	338 (4.75)	373	0.25	234 (78%)	
S-2-S	344 (4.60)	400	0.20	15 (58%)	
S-4-S	343 (4.67)	382	0.08	292 (93%)	
1-S-PTA	365 (4.52)	406	0.13	6	0.76
2-S-PTA	384 (4.67)	405	0.10	3	0.80
4-S-PTA	433 (4.16)	480	0.60	9	0.87

[a]Photophysical measurements in hexane (5.0×10^{-6} mol·L^{-1}); CV measurements in DCM (1.0×10^{-3} mol·L^{-1}). [b]λ_{abs} is the strong absorption peak appearing at the longest wavelength. [c]λ_{em} is the fluorescence peak appearing at the shortest wavelength, with $\lambda_{ex} = \lambda_{abs}$. [d]Determined using pyrene and coumarin 307 as references. [e]Decay curves were recorded at λ_{em} with $\lambda_{ex} = \lambda_{abs}$. [f]Values recorded vs Ag/AgCl.

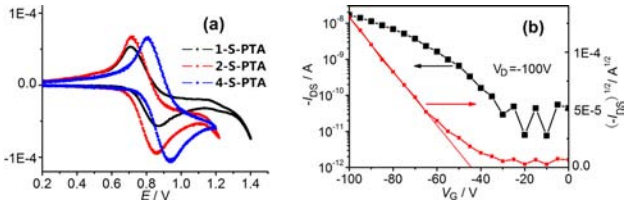

Figure 3. (a) Cyclic voltammetry spectrum of **PTAs** in CH_2Cl_2 solution (1.0×10^{-3} mol·L^{-1}) and (b) typical transfer characteristics of the transistor of **4-S-PTA**.

The properties of crystal OFETs of these **PTAs** were preliminarily examined. Typical transistor characteristics are shown in Figure 3b. The **PTAs** form large-scale ribbon-like crystals by drop-casting of DCM solutions (1.0 mg/mL) on octadecyltrichlorosilane (OTS)-treated SiO_2/Si substrates. The crystals were several micrometers in width and several tens to hundreds of millimers in length, as investigated in the optical microscopic images (Figure S-14, Supporting Information). Strong and sharp diffraction peaks appeared in the XRD results (Figure S-15, Supporting Information) were indexed by the corresponding single crystals, indicating that the molecular packing of all the ribbon-like crystals is consistent with the single-crystal structures. In order to inspect the charge transport property of **PTAs**, the crystalline ribbons were employed to prepare bottom-gate, top-contact field-effect transistors. The cleaning of the SiO_2/Si wafers and modification by OTS were performed according to reported processes.[18] The Au source and drain electrodes were fabricated through a "Au stripe mask". The measurement of the device was carried out under ambient conditions. Preliminary experiments show that single, ribbon-like crystals of **1-S-PTA**, **2-S-PTA**, and **4-S-PTA** have mobilities of 1.0×10^{-4}, 4.0×10^{-3}, and 2.1×10^{-3} cm^2/V s, respectively. Although the performance of **1-S-PTA** is moderate, the values of **2-S-PTA** and **4-S-PTA** are comparable with that of reported fused 4,5-dithienylpyrene.[7a]

The performance of organic micro-/nanosized ribbon transistors is strongly affected by the molecular packing in the ribbons (such as the molecular packing mode, $\pi-\pi$ overlap), the quality of the micro-/nanosized ribbons, and other factors (such as metal-semiconductor contacts, etc). The longest $\pi-\pi$ stacking distance and the smallest $\pi-\pi$ overlap is likely responsible for the lowest performance of **1-S-PTA** among these **PTA** isomers. The mobilities of **2-S-PTA** and **4-S-PTA** are in the same order of magnitude with a little variation, which might be ascribed to the difference in the quality of the ribbons (Figure S-14, Supporting Information). Improved device performance is expected by tuning the crystal growth condition and optimizing the updated device design.

In summary, three approaches to the synthesis of new sulfur-bridged multisubstituted pyrene derivative pyrene−thienoacenes were successfully developed. Extensive structural and photoelectronic measurements indicated that cyclization resulted in greatly enhanced intramolecular π-conjugation and intermolecular π-stacking, as well as transistor mobility. Among these regioisomeric **PTAs**, a [3,4]-extended isomer showed much more remarkable properties than [1,2]- and [2,1]-extended isomers. We believe this fundamental research will provide new insight for further work on sulfur-substituted fused pyrene derivatives for OFET application. Studies on multi-substituted and multisulfur containing pyrene−thienoacenes are underway in our group.

■ ASSOCIATED CONTENT

Supporting Information

Full experimental details, characterization data, DFT calculations, and CIF files for compounds **S-X-S** and **PTAs**.This material is available free of charge via the Internet at http://pubs.acs.org.

■ AUTHOR INFORMATION

Corresponding Authors

*E-mail: zqliu@sdu.edu.cn.
*E-mail: lhx@sioc.ac.cn.

Notes

The authors declare no competing financial interest.

dx.doi.org/10.1021/ol402971n | Org. Lett. 2014, 16, 342−345

■ ACKNOWLEDGMENTS

Financial support from the National Natural Science Foundation of China (20802026, 50803033, and 20972089) and the Independent Innovation Foundation of Shandong University is gratefully acknowledged.

■ REFERENCES

(1) (a) Figueira-Duarte, T. M.; Müllen, K. *Chem. Rev.* **2011**, *111*, 7260. (b) Crawford, A. G.; Dwyer, A. D.; Liu, Z.; Steffen, A.; Beeby, A.; Pålsson, L.-O.; Tozer, D. J.; Marder, T. B. *J. Am. Chem. Soc.* **2011**, *133*, 13349. (c) Edkins, R. M.; Fuce, K.; Peach, M. J. G.; Crawford, A. G.; Marder, T. B.; Beeby, A. *Inorg. Chem.* **2013**, *52*, 8942.

(2) Vollmann, H.; Becker, H.; Corell, M.; Streeck, H.; Langbein, G. *Justus Liebigs Ann. Chem.* **1937**, *531*, 1.

(3) Miura, Y.; Yamano, E.; Tanaka, A.; Yamauchi, J. *J. Org. Chem.* **1994**, *59*, 3294.

(4) (a) Coventry, D. N.; Batsanov, A. S.; Goeta, A. E.; Howard, J. A. K.; Marder, T. B.; Perutz, R. N. *Chem. Commun.* **2005**, *41*, 2172. (b) Crawford, A. G.; Liu, Z.; Mkhalid, I. A. I.; Thibault, M.-H.; Schwarz, N.; Alcaraz, G.; Steffen, A.; Collings, J. C.; Marder, T. B. *Chem.—Eur. J.* **2012**, *18*, 5022.

(5) Qiao, Y.; Zhang, J.; Xu, W.; Zhu, D. *Tetrahedron* **2011**, *67*, 3395.

(6) Hu, J.; Zhang, D.; Harris, F. W. *J. Org. Chem.* **2005**, *70*, 707.

(7) (a) Zöphel, L.; Beckmann, D.; Enkelmann, V.; Chercka, D.; Rieger, R.; Müllen, K. *Chem. Commun.* **2011**, *47*, 6960. (b) Zöphel, L.; Enkelmann, V.; Rieger, R.; Müllen, K. *Org. Lett.* **2011**, *13*, 4506. (c) Zöphel, L.; Enkelmann, V.; Müllen, K. *Org. Lett.* **2013**, *15*, 804.

(8) Mochida, K.; Kawasumi, K.; Segawa, Y.; Itami, K. *J. Am. Chem. Soc.* **2011**, *133*, 10716.

(9) (a) Venkataramana, G.; Dongare, P.; Dawe, L. N.; Thompson, D. W.; Zhao, Y.; Bodwell, G. J. *Org. Lett.* **2011**, *13*, 2240. (b) Ou, L.; Wang, X.-Y.; Shi, K.; Wang, J.-Y.; Pei, J. *Org. Lett.* **2013**, *15*, 4378. (c) Xiao, J.; Yang, B.; Wong, J. I.; Liu, Y.; Wei, F. X.; Tan, K. J.; Teng, X.; Wu, Y.; Huang, L.; Kloc, C.; Boey, F.; Ma, J.; Zhang, H.; Yang, H. Y.; Zhang, Q. *Org. Lett.* **2011**, *13*, 3004. (d) Jniko, Y.; Kawauchi, S.; Otsu, S.; Tokumaru, K.; Konishi, G. *J. Org. Chem.* **2013**, *78*, 3196. (e) Keller, S. N.; Veltri, N. L.; Sutherland, T. C. *Org. Lett.* **2013**, *15*, 4798.

(10) Zhou, Y.; Wang, F.; Kim, Y.; Kim, S.-J.; Yoon, J. *Org. Lett.* **2009**, *11*, 4442.

(11) (a) Freund, T.; Scherf, U.; Müllen, K. *Angew. Chem., Int. Ed.* **1995**, *33*, 2424. (b) Freund, T.; Scherf, U.; Müllen, K. *Macromolecules* **1995**, *28*, 547.

(12) (a) Takimiya, K.; Nakano, M.; Kang, M. J.; Miyazaki, E.; Osaka, I. *Eur. J. Org. Chem.* **2013**, 217. (b) Mori, T.; Nishimura, T.; Yamamoto, T.; Doi, I.; Miyazaki, E.; Osaka, I.; Takimiya, K. *J. Am. Chem. Soc.* **2013**, *135*, 13900.

(13) (a) Wang, C.; Dong, H. L.; Hu, W.; Liu, Y.; Zhu, D. *Chem. Rev.* **2012**, *112*, 2208. (b) Mei, J.; Diao, Y.; Appleton, A. L.; Fang, L.; Bao, Z. *J. Am. Chem. Soc.* **2013**, *135*, 6724.

(14) Rungtaweevoranit, B.; Butsuri, A.; Wongma, K.; Sadorn, K.; Neranon, K.; Nerungsi, C.; Thongpanchang, T. *Tetrahedron Lett.* **2012**, *53*, 1816.

(15) Sirringhaus, H.; Friend, R. H.; Wang, C.; Leuninger, J.; Müllen, K. *J. Mater. Chem.* **1999**, *9*, 2095.

(16) (a) Gao, P.; Beckmann, D.; Tsao, H. N.; Feng, X.; Enkelmann, V.; Pisula, W.; Müllen, K. *Chem. Commun.* **2008**, *44*, 1548. (b) Du, C.; Ye, S.; Liu, Y.; Guo, Y.; Wu, T.; Liu, H.; Zheng, J.; Cheng, C.; Zhu, M.; Yu, G. *Chem. Commun.* **2010**, *46*, 8573. (c) Gao, J.; Li, Y.; Wang, Z. *Org. Lett.* **2013**, *15*, 1366.

(17) Yamamoto, K.; Shouji, E.; Nishide, H.; Tsuchida, E. *J. Am. Chem. Soc.* **1993**, *115*, 5819.

(18) Wang, M.; Li, J.; Zhao, G.; Wu, Q.; Huang, Y.; Hu, W.; Gao, G.; Li, H.; Zhu, D. *Adv. Mater.* **2013**, *15*, 2229.